MODELING ALPINE SNOW HYDROLOGY IN THE CANADIAN ROCKY MOUNTAINS

John Pomeroy[1], Matt MacDonald [1], Chris DeBeer[1] and Tom Brown[2]

ABSTRACT

Field and modeling studies at Marmot Creek Research Basin in the Canadian Rocky Mountain have been directed to advance the understanding of snow processes and to improve hydrometeorological models of snowpack, streamflow and related atmospheric variables. Modeling studies of blowing snow over alpine terrain are showing promise in the prediction of the spatial distributions of snow water equivalent in complex environments. The model includes a complex terrain wind flow algorithm coupled to a two-phase flow snow transport and sublimation algorithm. It calculates snow accumulation as a residual of the snow redistribution and sublimation processes. An important new feature is the application of the model to aggregated landscape units (Hydrological Response Units or HRU) having common physiographic and aerodynamic characteristics; these landscape units require much less physiographic information than do fully spatially distributed blowing snow models and are suitable to application in remote alpine regions with sparse data. Comparisons of model outputs to snow surveys suggest that this level of spatial resolution and physically based simulation can produce reliable snow accumulation estimates in Canadian Rocky Mountain alpine catchments. Snow ablation studies have focussed on application of the energy balance to estimate snowmelt over landscape units with consideration of sub-unit depletion of snow covered area. In this case hydrological response units are segregated based on snow accumulation characteristics and applied melt energy fluxes. The calculated melt rates agree well with observations snow surveys. Improved algorithms resulting from this application of field technology are being used to update a modular, object-oriented computer simulation of the cold regions hydrological cycle, the Cold Regions Hydrological Model, CRHM. CRHM can be easily and frequently updated as improved algorithms become available and used to predict both snow dynamics and streamflow from high mountain areas. (Keywords: blowing snow, snowmelt, snow covered area depletion, hydrological modeling)

INTRODUCTION

The Canadian Rocky Mountains provide a substantial proportion of flow for the eastward flowing Saskatchewan and northward flowing Athabasca River systems. These rivers provide crucial water supplies to agricultural and oil sand development regions of Alberta and Saskatchewan as well as the primary municipal supply for Calgary, Edmonton, Saskatoon and Regina and other communities. They also support spectacular and important aquatic ecosystems in the rivers, wetlands and lakes of the Athabasca-Mackenzie and Saskatchewan-Nelson drainages and provide freshwater to the Arctic Ocean and Hudson Bay. Snowmelt provides the vast majority of runoff from the Rocky Mountains, with most snowmelt being released at high elevations from April through July; concomitant with peak streamflow in June. Unfortunately streamflow in the region is generally declining with time (Stewart et al., 2004; Valeo et al., 2007); an example is the Bow River at Banff which has lost 11.5% of its mean annual flow over the period 1910 to 2004 (Figure 1). This trend is statistically significant at the 99% level according to the Mann-Kendall test (Harder, 2008). The decline in summer flows is even more severe than the annual trend, with a 24.8% decline in the August streamflow of the Bow River since the early 20th century.

This change in mountain water resources means that we must better understand mountain snow processes and endeavour to predict them in a robust, physically based manner that will be useful for future conditions. Much of the runoff producing zone of the Rockies is the alpine zone, above treeline. Here the major snow processes are wind redistribution and sublimation by blowing snow and snowmelt. Wind redistribution occurs over much of the winter and has been noted in the region for many years (Church, 1933). Snowmelt occurs during a period of high precipitation in May through July and precipitation may occur as rain or snowfall. Alpine basins have a long period in which they are partially snowcovered. The snowcovered area controls the contributing area for runoff generation from snowmelt and so is an important hydrological state variable for runoff prediction. Clear periods are also common during melt, leading to substantial differences in melt rate with slope and aspect, and south facing slopes

Paper presented Western Snow Conference 2009
[1] Centre for Hydrology, University of Saskatchewan, 117 Science Place, Saskatoon, Sask. Canada, S7N 5C8
www.usask.ca/hydrology, john.pomeroy@usask.ca

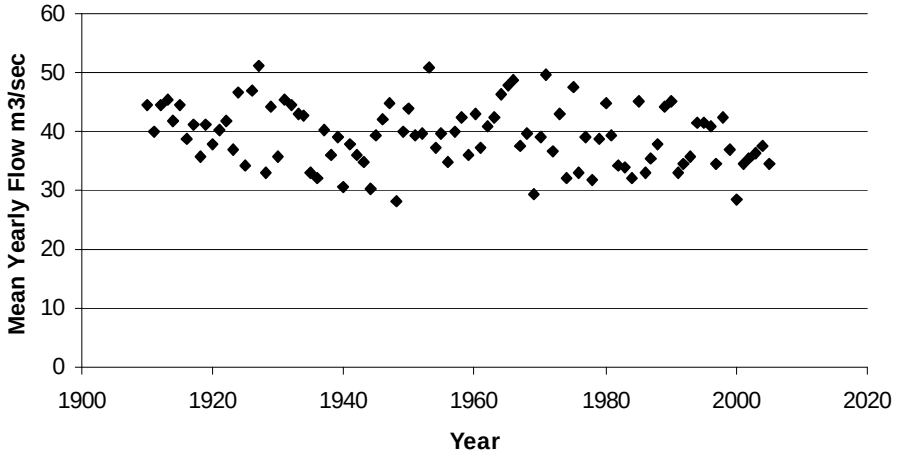

Figure 1. Mean annual flow of the Bow River at Banff.

becoming snowfree many weeks before north faces (DeBeer and Pomeroy, 2009). The challenge is to model the accumulation and ablation of snow in such a complex and dynamic environment. The purpose of this paper is to outline and demonstrate a procedure for calculating snow accumulation and ablation in headwater basins of the Canadian Rockies.

STUDY SITE AND OBSERVATIONS

Simulations of snow transport and sublimation by wind, and snowmelt were performed and evaluated over a 6,000 m^2 section of an alpine ridge, known as Fisera Ridge, in the headwaters of the Marmot Creek Research Basin (50°57' N, 115°10' W). Fisera Ridge is located at the treeline, where subalpine fir and larch give way to sparse shrubs, exposed soils and grasses. The north-facing slope and ridge-top of the ridge are generally windswept and the south-facing slope and down-wind forested area are snow deposition zones.

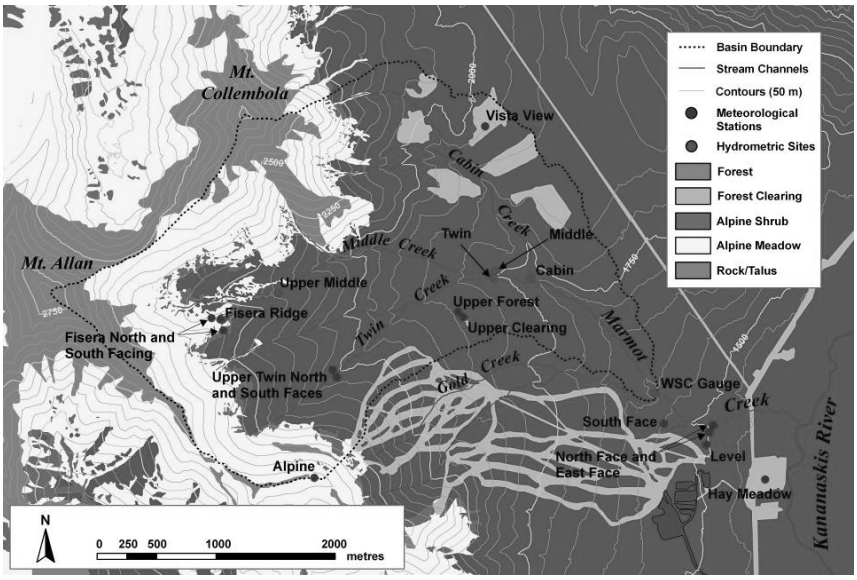

Figure 2. Marmot Creek Research Basin, Alberta showing land cover and observation sites.

Meteorological observations from three meteorological stations located at Fisera Ridge from the winter 2007-2008 and spring-summer 2007 were used. Precipitation data from a Geonor T-200B accumulating precipitation gauge located in a forest clearing at lower elevation (1853 m ASL) in the Marmot Creek Research Basin was used. Due to elevation effects, the recorded precipitation values were increased for application at FR according to observations present by Auld (1995). Table 1 presents a summary of meteorological observations during the winter period.

Only the ablation period of 2007 was used to test melt simulations. Figure 3 presents air temperature and daily precipitation during the spring ablation period.

Table 1. Summary of meteorological conditions during the winter simulation period (October 2007-April 2008)

Mean temperature (°C)	Mean Relative Humidity (%)	Mean North-facing Wind Speed ($m\ s^{-1}$)	Mean Ridge-top Wind Speed ($m\ s^{-1}$)	Mean South-facing Wind Speed ($m\ s^{-1}$)	Mean Ridge-top Downwelling Shortwave Radiation ($W\ m^{-2}$)	Mean Ridge-top Downwelling Longwave Radiation ($W\ m^{-2}$)	Total Precipitation (mm)
-7.6	68	3.9	3.3	2.5	63	221	320

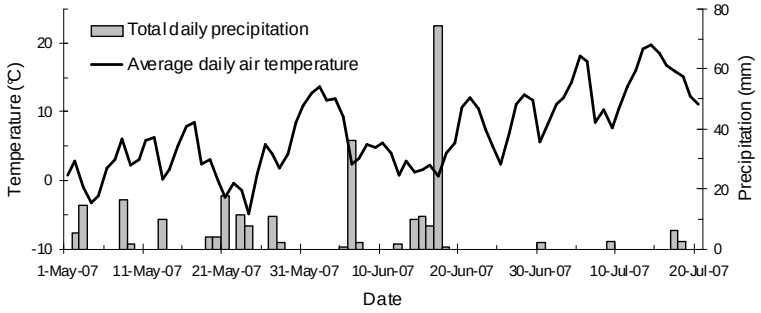

Figure 3. Precipitation and air temperatures at Fisera Ridge during the ablation period (May-July 2007)

Snow surveys consisted of a total of 155 points along a transect from north to south facing slope and along the ridgetop. Depth measurements were taken every 3m, while snow density measured using an ESC30 snow tube if the snow depth was below 120cm, otherwise density measurements from snow pits adjacent to snow survey transects were used.

MODELING METHODOLOGY

Model Description

Simulations were performed using the Cold Regions Hydrological Modeling Platform (CRHM; Pomeroy et al., 2007). CRHM has a modular, object-oriented structure whereby the user specifies which physically-based algorithms (known as modules) are used to simulate hydrological processes. An attempt was made to select the most appropriate modules available for the simulations required. For the winter snow redistribution and sublimation calculations a blowing snow module was coupled with a simple single-layer daily energy balance snowmelt module. For the spring snowmelt simulations a sophisticated layered half-hourly energy balance snowmelt module was coupled with a snowcovered area depletion model.

The snow mass balance of a uniform landscape element is a result of snowfall accumulation, the distribution and divergence of blowing snow fluxes both within and surrounding the element, sublimation and snowmelt as

$$\frac{dS}{dt}(x) = P - p\left[\nabla F(x) + \frac{\int E_B(x)dx}{x}\right] - E - M$$

1)

where *dS/dt* is surface snow accumulation (kg m^{-2} s^{-1}), *P* is snowfall (kg m^{-2} s^{-1}), *p* is the probability of blowing snow occurrence, *F* is the snow transport rate (kg m^{-1} s^{-1}), E_B is blowing snow sublimation (kg m^{-2} s^{-1}), *x* is fetch (m), *E* is the snow surface sublimation (kg m^{-2} s^{-1}) and *M* is snowmelt (kg m^{-2} s^{-1}).

The snow transport and sublimation terms were simulated using the Prairie Blowing Snow Model (PBSM; Pomeroy et al., 1993; Pomeroy and Li, 2000). PBSM calculates two-dimensional blowing snow transport and sublimation rates for steady-state conditions over a landscape using mass and energy balances. PBSM was initially developed for application over the Canadian Prairies, characterized by relatively flat terrain and homogeneous crop cover (Pomeroy et al., 1993). Versions have been applied over alpine tundra (Pomeroy, 1991) and arctic tundra (Pomeroy and Li, 2000).

Snowmelt, *M*, in mid-winter was simulated using the Energy-budget Snowmelt Model (EBSM; Gray and Landine, 1988) and during the melt period by Snobal (Marks et al., 1998). EBSM calculates the amount of snowmelt using the energy equation and is appropriate for cold weather and shallow snow simulations. It couples with PBSM in a stable manner. Snowbal is more appropriate for the seasonal melt of deep snowpacks where large energy inputs, precipitation during melt, and liquid water retention are important to snowmelt dynamics. The amount of snowmelt was calculated using

$$M = \frac{Q_m}{\rho h_f B} \qquad 2)$$

where Q_m is the energy available for melt, ρ is the density of water, h_f is the latent heat of fusion (333.5 kJ kg^{-1})and *B* is the thermal quality of snow or the fraction of ice in a unit mass of wet snow (0.95-0.97). Q_m is calculated from the energy equation as

$$Q_m = Q_{sn} + Q_{\ln} + Q_h + Q_e + Q_g + Q_p - {du}/{dt} \qquad 3)$$

where Q_{sn} is net shortwave radiation absorbed by the snowpack, Q_{ln} is net longwave radiation at snow surface, Q_h is the sensible heat flux, Q_e is the latent heat flux, Q_g is the ground heat flux by conduction, Q_p is the energy flux from rain by advection, and *du/dt* is the rate of changes in internal energy.

Incoming solar radiation was partitioned into direct and diffuse components (K_{dir} and K_{diff}, respectively) using expressions by Garnier and Ohmura (1970). K_{dir} and K_{diff} were partitioned using a cloudiness index calculated from the relation between observed incoming shortwave radiation and the theoretical clear-sky solar radiation over flat areas. Incoming solar radiation was adjusted for aspect and slope, presuming the same cloudiness index for each slope.

Snow albedo, α, during winter (EBSM) was estimated using the method outlined by Gray and Landine (1987). Snow surface albedo during the seasonal melt period (Snobal) was estimated using an exponential decay to an asymptotic minimum of 0.3 following Essery and Etchevers (2004). For each timestep with snowmelt, the albedo was updated according to:

$$\alpha \rightarrow (\alpha - 0.3)\exp\left(\frac{-\Delta t}{\tau}\right) + 0.3 \qquad 4)$$

where Δt is the timestep length and τ is a time constant applied to melting snow (10^6 seconds). For time steps with snowfall, the albedo was increased by:

$$\alpha \rightarrow \alpha + (\alpha_f - \alpha)\frac{S_f \Delta t}{10} \qquad 5)$$

where S_f is the snowfall rate (mm/Δt), so that a 10 mm snowfall refreshes the albedo to α_f (set equal to 0.85).

Incoming longwave radiation was adjusted for slopes using a modified version of the parameterization suggested by Sicart et al. (2006), in which the effect of varying sky view is accounted for. The sky view factor is the fraction of sky visible from a specific point, and is defined as the ratio of the projected area of the visible

hemisphere to the projected area of the whole hemisphere. Longwave irradiance on the slopes, Q_l, was calculated as:

$$Q_l = Q_{l_0} + V_{eff}\varepsilon_s\sigma T_s^4, \quad 6)$$

where Q_{l0} is the observed incoming longwave radiation, V_{eff} is the effective terrain view factor (i.e. the difference between sky view factor at the observation site and that over the slope), ε_s is the emissivity of the surface (taken as 0.98), σ is the Stefan-Boltzmann constant (5.67×10^{-8} W m^{-2} K^{-4}), and T_s is the surface temperature (K). The daily average air temperature was taken as an approximation of the surface temperature. The parameter V_{eff} accounts for the fact that a component of the observed longwave radiation is contributed from adjacent terrain. This parameter effectively represents the relative increase (or decrease) in exposure to surrounding terrain, and thus provides a useful means for extrapolating longwave radiation measurements to nearby locations with different sky view factors. To obtain representative values of sky view factor, several digital hemispheric photographs were taken. Sky view factor was then calculated from these images, following Corripio (2003), as r^2/R^2, where r is the average radius of the visible horizon, and R is the radius of the image.

Model Parameterisation

A landscape-based aggregated approach was employed for the alpine following principles outlined by Stepphun and Dyck (1974), MacDonald et al. (2009) and DeBeer and Pomeroy (2009). Five hydrological response units (HRU) were used to define landscape units for simulating winter snow redistribution over Fisera Ridge (Figure 4): North-facing slope (NF), Ridge-top (Ridge), Upper Southeast-facing slope (SEF Upper), Lower Southeast-facing slope (SEF Lower) and Forest. These five HRUs were selected based on consideration of the landscape features that govern alpine snow redistribution and ablation at small scales, chiefly sun exposure, wind exposure and vegetation cover. Under normal wind directions, deposited snow is scoured from the NF and Ridge and deposited into the SEF Upper, SEF Lower and Forest. SEF Lower is located in a clearing with low wind speed compared to SEF Upper; for this reason, snow transport was inhibited from occurring from SEF Lower.

For snowmelt, the five HRU were aggregated to three HRU representing the Ridge, SEF and NF. These three HRU represented the main elements for snowmelt modeling to consider: differing end-of-winter SWE and differing incoming energy due to slope. The forest HRU was not considered for alpine melt modeling.

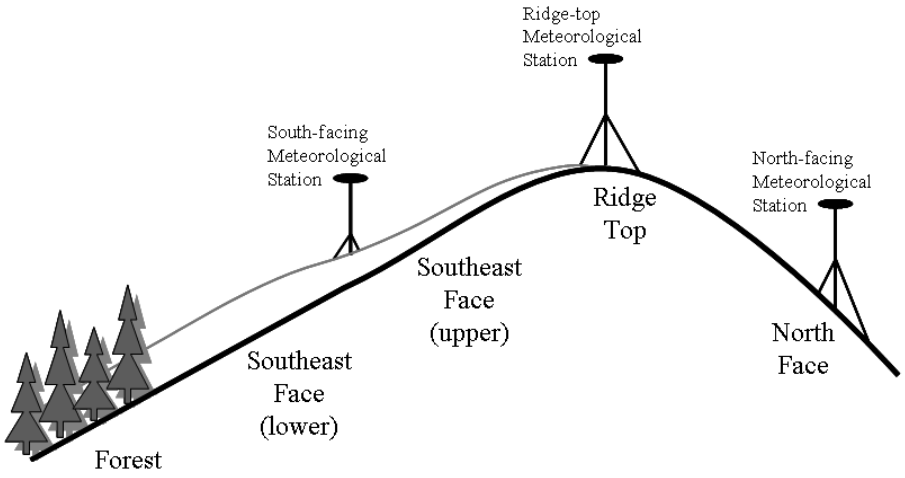

Figure 4. Fisera Ridge Hydrological Response Units (not to scale).

RESULTS

Figure 5 shows measured cumulative snowfall and both measured and simulated snow accumulation for each HRU from the period 20 October to 30 April. Snow redistribution from the NF and Ridge HRU is indicated by SWE being only 1/3rd of cumulative snowfall at these sites. Snow accumulation at SEF Upper approximately

equalled cumulative snowfall suggesting little net redistribution of snow. Snow redistribution to the SEF Lower and Forest HRU is indicated by SWE being more than double the cumulative snowfall. Simulated cumulative blowing snow sublimation as a fraction of cumulative snowfall was 63%, 35% and 0.2% for the NF, Ridge and SEF Upper, respectively. The area-weighted blowing snow sublimation as a fraction of cumulative snowfall for all of Fisera Ride was 36%. The simulation was performed during a period of little snowmelt, as the cumulative winter snowmelt was calculated to be 2.4 mm over all HRUs.

There was good agreement between observed and modelled SWE in the winter. The most notable disagreements were overestimated SWE on the SEF Upper and SEF Lower by 23 mm and 43 mm, respectively, in February and then underestimated by 62 mm and 44 mm, respectively, in April. Comparisons of modelled to measured values over the whole measurement period indicate a Modified Nash-Sutcliffe (MNS) statistic of 0.98; a value of 1.0 would indicate perfectly simulated SWE and a value of 0 would indicate that simulated SWE is only as accurate as that estimated by using accumulated snowfall only (i.e. not using a blowing snow model). The mean bias (MB) is the fraction that the model overestimates or underestimates SWE, the calculated value of -0.05 shows a small underestimation. The root mean square error (RMSE) is the average magnitude of the error in simulated snow accumulation in mm SWE and at 7.3 mm is about 2.4% of cumulative snowfall.

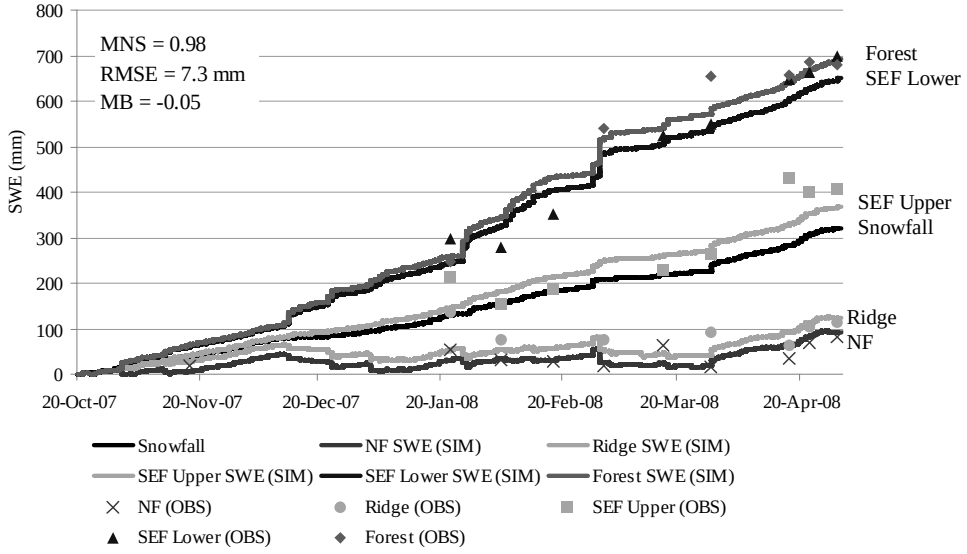

Figure 5. Observed and simulated snow accumulation, Fisera Ridge. Observations are averaged values from snow survey transects. Simulations are CRHM daily outputs from a coupled blowing snow and snowmelt calculation.

Figure 6 shows both the modelled and observed SWE at the Fisera Ridge meteorological station during the melt period of 2007. SWE was modelled for this test case using an initial value of 170 mm SWE depth beginning on 1-April. Observed SWE values were derived from the measurements of snow depth obtained from an acoustic snow depth gauge (SR50), together with measured snow density at several times throughout the melt period and modelled density for the intervening periods. The model clearly performs well for the simulation of snowmelt, as it accurately represents the timing of both melt onset and snow disappearance, and conforms well to the observed melt rates at all times during the snowmelt period. The model also performs reasonably well in simulating snow accumulation. The RMSE error between modelled and observed SWE (excluding times when SWE = 0) was 18.9 mm or about 11% of the initial SWE. The evaluation of the model at a point confirms that it is suitable for simulations of snowmelt at Fisera Ridge.

Simulations of melt rate on the NF and SEF HRUs show substantially higher melt rates on the SF in early melt (May) with differences becoming smaller by June (Figure 7). The greater melt rates on the SF are due to greater insolation to the south-facing slope. This is partly compensated by greater longwave irradiance to the north facing slope because of its smaller sky view area. Slope-based melt rate differences are enhanced in early melt by relatively warm snowpack temperatures on south-facing slopes and cold snowpacks on north faces. As melt progresses, the internal energy states of all snowpacks become more similar and tend towards isothermal conditions. Hence the differences in melt rate in early melt are due to cumulative energy inputs over the winter, which were greater to the south-facing slopes.

The melt rates calculated in this modeling approach can be used to drive a snow covered area depletion model as shown by DeBeer and Pomeroy (2009) if the initial SWE and its coefficient of variation are known. Such a model can calculate areal melt rates that are useful for hydrological simulations. The end of winter SWE is estimated from the blowing snow model and melt simulations for mid-winter which then provide the initial conditions for the spring/summer melt simulations. The coefficient of variation is a generally stable value from year to year and can be estimated from local snow surveys or chosen for the landscape type from many archived values in the literature (e.g. Pomeroy et al., 1998; 2004).

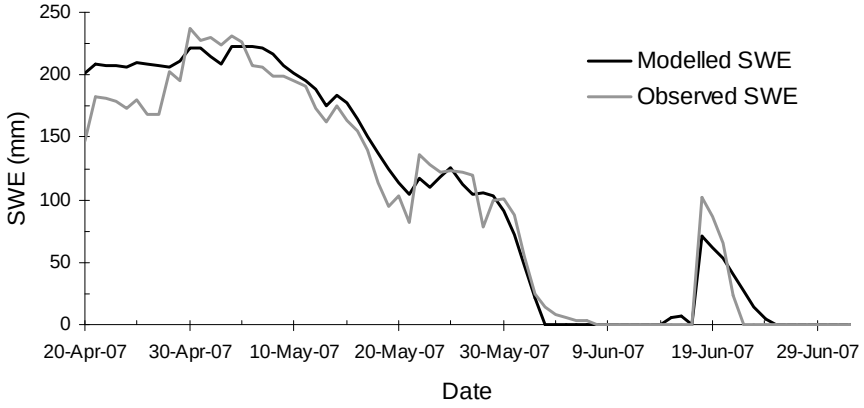

Figure 6. Observed and modeled SWE during ablation season at the Fisera Ridge ridgetop site, 2007.

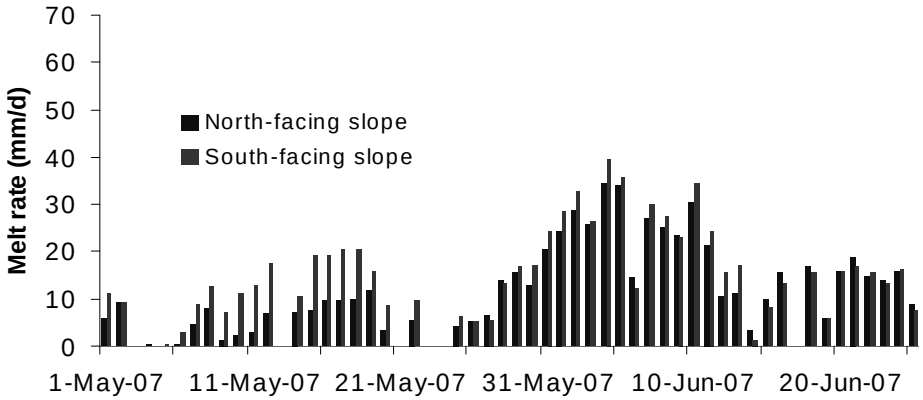

Figure 7. Modelled melt rates on south facing and north facing slopes of Fisera Ridge during the ablation season

CONCLUSIONS

Alpine snow in the Canadian Rockies is subject to substantial wind redistribution and sublimation losses during the winter and then melt in spring and summer driven by radiation energy inputs. At Marmot Creek winter wind redistribution is from wind-scoured north facing slopes and ridge-tops to sheltered south facing slopes and

tree-line forests, with end of winter accumulation on sheltered sites being eight times greater than on the wind-scoured sites. Blowing snow sublimation losses over an alpine transect were substantial and totaled 36% of winter snowfall. Mid-winter melt was minimal. Spring snowmelt rates were greater on the south-facing slopes than on north-facing slopes in early melt periods, but these differences became smaller in June as internal energy deficits in the snowpacks become small.

Snow dynamics in this alpine environment can be calculated by using a system of radiation loading, blowing snow transport and sublimation, and energy balance snowmelt calculations applied to hydrological response units in the Cold Regions Hydrological Model. Simulations using algorithms in this model were able to successfully match observed snow accumulation and ablation dynamics over an alpine ridge and can be applied to larger areas using the hydrological response unit approach. Crucial to the success of this modeling was having a high quality meteorological stations on site in a high alpine environment. Challenges remain in estimating the driving meteorology for such detailed physical calculations in alpine regions given the sparse meteorological observation network at high elevations and uncertainties in atmospheric model products.

ACKNOWLEDGEMENTS

The authors would like to acknowledge the assistance of Mike Solohub, Chad Ellis, Anne Sabourin, James MacDonald, Richard Essery and others in the field. The financial support of NSERC, CFCAS (IP3), and the Canada Research Chair programme is gratefully acknowledged. Logistical support from the University of Calgary Biogeoscience Institute and the Nakiska Ski Resort, Kananaskis greatly aided this study.

REFERENCES

Auld, H. 1995. Dependence of ground snow loads on elevation in western Canada. Proceedings of theWestern Snow Conference 63:143-146.

Corripio, J. G. 2003. Vectorial algebra algorithms for calculating terrain parameters from DEMs and solar radiation modeling in mountainous terrain. International Journal of Geographic Information Science, 17:1–23.

Church, J.E. 1933. Snow surveying: its principles and possibilities. Geographical Review 23(4):529-563.

DeBeer, C.M. and J.W. Pomeroy. 2009. Modeling snowmelt and snowcover depletion in a small alpine cirque, Canadian Rocky Mountains. Hydrological Processes, DOI:10.1002/hyp.7346.

Essery, R., and P. Etchevers. 2004. Parameter sensitivity in simulations of snowmelt. Journal of Geophysical Research, 109: D20111, doi:10.1029/2004JD005036.

Garnier, B.J. and A. Ohmura. 1970. The evaluation of surface variations in solar radiation income. Solar Energy, 13:21–34.

Gray, D.M. and P.G. Landine. 1987. Albedo model for shallow prairie snow covers. Canadian Journal of Earth Sciences 24:1760-1768.

Gray, D.M. and P.G. Landine. 1988. An energy-budget snowmelt model for the Canadian Prairies. Canadian Journal of Earth Sciences 25:1292-1303.

Harder, P. 2008. Hydroclimatological Trends in the Kananaskis Valley. Centre for Hydrology Internal Report, University of Saskatchewan, Saskatoon.

MacDonald, M.K., J.W. Pomeroy, and A. Pietroniro. 2009. Parameterising redistribution and sublimation of blowing snow for hydrological models: tests in a mountainous subarctic catchment. Hydrological Processes, DOI:10.1002/hyp.7356.

Marks, D., J. Kimball, D. Tingey, and T. Link. 1998. The sensitivity of snowmelt processes to climate conditions and forest cover during rain-on-snow: a case study of the 1996 Pacific Northwest flood. Hydrological Processes, 12:1569–1587.

Pomeroy, J.W. 1991. Transport and sublimation of snow in wind-scoured alpine terrain. In (eds. H Bergman, H Lang, W Frey, D Issler, B Salm) Snow, Hydrology and Forests in Alpine Areas. International Association of Hydrological Sciences Publication No. 205. Wallingford, UK: IAHS Press. 131-140.

Pomeroy, J.W, D.M. Gray, and P.G. Landine. 1993. The Prairie Blowing Snow Model: characteristics, validation and operation. Journal of Hydrology, 144:165-192.

Pomeroy, J.W., D.M. Gray, K.R. Shook, B. Toth, R.L.H. Essery, A. Pietroniro, and N. Hedstrom. 1998. An evaluation of snow accumulation and ablation processes for land surface modeling. Hydrological Processes, 12: 2339-2367.

Pomeroy, J.W. and L. Li. 2000. Prairie and arctic areal snow cover mass balance using a blowing snow model. Journal of Geophysical Research-Atmospheres, 105: 26619-26634.

Pomeroy, J. W., R.L.H. Essery, and B. Toth. 2004. Implications of spatial distributions of snow mass and melt rate for snow-cover depletion: observations in a subarctic mountain catchment. Annals of Glaciology, 38: 195–201.

Pomeroy, J.W., D.M. Gray, T. Brown, N.R. Hedstrom, W.L. Quinton, R.J. Granger, and S.K. Carey. 2007. The cold regions hydrological model: a platform for basing process representation and model structure on physical evidence. Hydrological Processes, 21:2650-2667.

Sicart, J.E., J.W. Pomeroy, R.L.H. Essery, and D. Bewley. 2006. Incoming longwave radiation to melting snow: observations, sensitivity and estimation in northern environments. Hydrological Processes, 20: 3697–3708.

Steppuhn, H.W. and G.E. Dyck. 1974. Estimating true basin snowcover. Advanced Concepts in Technical Study of Snow and Ice Resources, Interdisciplinary Symposium, U.S. National Academy of Science, Washington, D.C., pp. 314–328.

Stewart, I. T., D.R. Cayan, and M.D. Dettinger. 2004. Changes toward earlier streamflow timing across western North America. Journal of Climate, 18:1136-1155.

Valeo, C., Z. Xiang, F.J. Bouchart, P. Yeung and M.C. Ryan. 2007. Climate Change Impacts in the Elbow River Watershed. Canadian Water Resources Journal, 32 (4):285-302.